J. Adv. Model. Earth Syst., **Vol. 3**, M12002, 12 pp.

The family of anisotropically scaled equatorial waves

Enver Ramírez Gutiérrez[1,2], *Pedro Leite da Silva Dias*[1,3], *Carlos Raupp*[1] *and Jose Paulo Bonatti*[4]

[1] Departamento de Ciências Atmosféricas, IAG, USP, Rua do Matão, 1226, São Paulo, 05508-090, Brasil
[2] Centro de Ciência do Sistema Terrestre, CCST, INPE, Cachoeira Paulista, Brasil
[3] Laboratorio Nacional de Computação Cientifica, LNCC, Petrópolis, Brasil
[4] Centro de Previsão do Tempo e Estudos Climáticos, CPTEC, INPE, Rodovia Presidente Dutra, km 40, Cachoeira Paulista, 12630-000, Brasil

Manuscript submitted 15 April 2011

In the present work we introduce the family of anisotropic equatorial waves. This family corresponds to equatorial waves at intermediate states between the shallow water and the long wave approximation model. The new family is obtained by using anisotropic time/space scalings on the linearized, unforced and inviscid shallow water model. It is shown that the anisotropic equatorial waves tend to the solutions of the long wave model in one extreme and to the shallow water model solutions in the other extreme of the parameter dependency. Thus, the problem associated with the completeness of the long wave model solutions can be asymptotically addressed. The anisotropic dispersion relation is computed and, in addition to the typical dependency on the equivalent depth, meridional quantum number and zonal wavenumber, it also depends on the anisotropy between both zonal to meridional space and velocity scales as well as the fast to slow time scales ratio. For magnitudes of the scales compatible with those of the tropical region, both mixed Rossby-gravity and inertio-gravity waves are shifted to a moderately higher frequency and, consequently, not filtered out. This draws attention to the fact that, for completeness of the long wave like solutions, it is necessary to include both the anisotropic mixed Rossby-gravity and inertio-gravity waves. Furthermore, the connection of slow and fast manifolds (distinguishing feature of equatorial dynamics) is preserved, though modified for the equatorial anisotropy parameters used $\delta \in \langle 0,1]$. New possibilities of horizontal and vertical scale nonlinear interactions are allowed. Thus, the anisotropic shallow water model is of fundamental importance for understanding multiscale atmosphere and ocean dynamics in the tropics.

DOI:10.1029/2011MS000078

1. Introduction

Recently, there has been increased attention to multi-scale dynamics for atmosphere/ocean problems [*McWilliams and Gent*, 1978, 1980; *Zebiak*, 1982; *Gill and Phlips*, 1986; *Schopf and Suarez*, 1990; *Majda and Klein*, 2003; *Biello and Majda*, 2005; *Klein and Majda*, 2006; *Khouider and Majda*, 2006, 2007; *Raupp and Silva Dias*, 2009; *Ramírez Gutiérrez and Silva Dias*, 2009]. Multi-scale dynamics constitutes a powerful tool for understanding some key aspects of complex systems that involve many physical and dynamical processes. In atmosphere-ocean problems the relevant phenomena are organized in a wide, although well defined, spectrum of time and space scales (e.g., Pacific Decadal Oscillation (PDO), El Niño, the Madden-Julian oscillation, etc), some of which are still poorly understood. Consequently, it is difficult to conclude why the state-of-the-art complex models are still having problems in the prediction and simulation of some key features of these multi-scale phenomena. The tropical region is an important component of the earth system; it is in that region of the globe where most of the solar radiation is incident. The temperature gradients are weak and, unlike midlatitude dynamics, where baroclinic instability is the main energy source for large-scale weather systems, the scale-interactions involving clouds, moisture and coupling to the ocean play the major role in generating synoptic and planetary wave disturbances in the tropics [*Majda and Klein*, 2003; *Majda*,

To whom correspondence should be addressed.
P. L. da Silva Dias, E. Ramírez Gutiérrez, and C. Raupp, Departamento de Ciências Atmosféricas, IAG, USP, Rua do Matão, 1226, São Paulo, 05508-090, Brasil.
(enver.ramirez@gmail.com)

2007]. The degeneracy of the Coriolis force at the equator leads to the behavior of this region as a wave guide [*Matsuno*, 1966]. The β-plane long wave approximation is one of the simplest tools to capture the trapping behavior of the wave guide. However, the long wave approximation fails to give us a complete set of solutions and, consequently, it is limited for multiscale nonlinear interaction studies. In the present work, anisotropic scalings are used in the equatorial β-plane shallow water equations. These scalings exploit the fact that the wave guide is elongated in the east-west direction. Thus there exists an anisotropy between the zonal (u) and meridional (v) components of the velocity field. When the ratio $(v/u)\rightarrow 0$, the long wave approximation emerges. *Gill* [1980] used the long wave approximation to obtain some simple forced solutions in the equatorial primitive equations, and showed that the Kelvin and non-dispersive Rossby waves are the eigensolutions of the long wave approximation. However, the completeness of these solutions has not been proved. In addition, experience tells us that the ratio v/u is in general small but not so close to zero for large to planetary scale tropical phenomena [e.g., *Schubert et al.*, 2009]. Thus, it appears necessary to understand the equatorial wave dynamics at intermediate states between the shallow water and the long wave approximation and to analyze the completeness of the solutions. Precisely, *Ramírez Gutiérrez et al.* [2011] analyzed the nonlinear three-wave interaction in the anisotropically scaled equatorial β-plane shallow-water equations using moderate values of the anisotropy parameter. In their approach, the dispersion properties as well as the spatial structure of the equatorial wave modes were assumed to be unaffected by the anisotropy parameter, with the anisotropy modifying only the nonlinear interactions among the isotropic eigenmodes. They showed that for a given resonant triad, the nonlinear energy exchange is longer in the long wave regime than in the shallow water one. These results were confirmed independently in both theoretical and numerical frameworks.

In the present work, we extend the results of *Ramírez Gutiérrez et al.* [2011] by considering the modifications of the dispersion properties of the equatorial waves by the anisotropy of the spatial scales in the equatorial waves. For this purpose, we introduce in the equatorial β-plane shallow-water equations an anisotropy parameter (δ), which is a measure of both the meridional to zonal velocity and spatial scale ratio, as well as a measure of the fast to slow time scale ratio (for simplicity they are taken to be equal). Then, the linearized anisotropic shallow water model is solved. New dispersion curves are obtained for the Kelvin, Rossby, mixed Rossby-gravity and inertio-gravity waves. Implications of this δ dependency for the completeness of the eigensolutions is discussed in section 4. The anisotropic shallow water model, or equivalently the long wave like approximation, is more likely to occur in the tropical region.

2. Governing Equations

We begin with the nonlinear, unforced and inviscid shallow water equations on the equatorial β plane in their dimensional form, as given by

$$\partial_t u + \mathbf{v}\cdot\nabla u - \beta y v + g\partial_x H = 0, \tag{1a}$$

$$\partial_t v + \mathbf{v}\cdot\nabla v + \beta y u + g\partial_y H = 0, \tag{1b}$$

$$\partial_t H + \mathbf{v}\cdot\nabla H + H\nabla\cdot\mathbf{v} = 0, \tag{1c}$$

where $H=\bar{H}+\eta$, with $\bar{H}$ the mean thickness of the fluid layer and η the thickness perturbation due to wave activity. For the atmosphere it is common to use the approximation $\phi = g\eta$, where ϕ is the geopotential perturbation. *Ripa* [1983a] discussed an appropriate expression for η in both atmospheric and oceanic models. The equatorial Coriolis parameter is represented by βy. The equations can be nondimensionalized by using units of length and time according to

$$L=(C/\beta)^{1/2},\ T=(C\beta)^{-1/2}, \tag{2}$$

where C is either the atmospheric or oceanic first baroclinic wave speed defined in Table 1. It must be noted that there exist other definitions for the length and time scales in use, for instance: $R=(2C/\beta)^{1/2}; \tilde{\omega}=C/R=(C\beta/2)^{1/2}$. It can be easily verified that $\tilde{\omega}^{-1}\sim T$ and $R\sim L$ (in fact $\tilde{\omega}^{-1}=\sqrt{2}T, R=\sqrt{2}L$). Other forms in use are $2\pi R$ and $2\pi\tilde{\omega}^{-1}$. Although any of these leave invariant the ratio L/T, the precise definition of the time and space units changes the magnitudes of the scalings.

Using (2) we obtain the nondimensionalized and scaled variables given in (3), and also given by, e.g., *Pedlosky* [1987], *Dijkstra* [2000], and *Majda* [2002]. Note that as δ varies in the range $0<\delta\leq 1$, the zonal coordinate and time are large scale and slow time scale respectively, whereas the meridional velocity is diminished by the scaling.

$$\begin{gathered} x'=(L/\delta)x;\ y'=Ly;\ t'=(T/\delta)t; \\ u'=Cu;\ v'=\delta Cv;\ H'=(C^2/g)H;\ \eta'=\eta. \end{gathered} \tag{3}$$

Dropping the primes, the system of equations (1) with the anisotropic scalings becomes

$$\partial_t u + u\partial_x u + v\partial_y u - yv + \partial_x\eta = 0, \tag{4a}$$

Table 1. Typical Values of the First Baroclinic Gravity Wave Speed C, Mean Thickness of the Fluid Layer $\bar{H}$, Rossby Deformation Radius L and Time Scale T

	C (m/s)	$\bar{H}$ (m)	L (km)	T (hours)
atmosphere	50	250	1507.6	8.3
ocean	2.2	0.49	316.23	39.9

$$\delta^2\left[\partial_t v + u\partial_x v + v\partial_y v\right] + yu + \partial_y \eta = 0, \tag{4b}$$

$$\partial_t \eta + u\partial_x \eta + v\partial_y \eta + (1+\eta)\left(\partial_x u + \partial_y v\right) = 0. \tag{4c}$$

3. The δ-Modified Equatorial Waves

Linearization around a motionless basic state and the assumption of traveling wave solutions of the form $e^{i(kx-\omega t)}$, with k and ω representing zonal wavenumber and frequency respectively, yields the following eigenvalue problem for the meridional structure:

$$-i\omega\hat{u} - y\hat{v} + ik\hat{\eta} = 0, \tag{5a}$$

$$-\delta^2 i\omega\hat{v} + y\hat{u} + \partial_y\hat{\eta} = 0, \tag{5b}$$

$$-i\omega\hat{\eta} + ik\hat{u} + \partial_y\hat{v} = 0. \tag{5c}$$

It is possible to re-write the eigenvalue problem given by (5) in the matrix form

$$\begin{pmatrix} -i\omega & -y & ik \\ y & -\delta^2 i\omega & \partial_y \\ -ik & \partial_y & -i\omega \end{pmatrix}\begin{pmatrix} \hat{u} \\ \hat{v} \\ \hat{\eta} \end{pmatrix} = 0. \tag{6}$$

Solving the matrix

$$\begin{pmatrix} 0 & \dfrac{\partial_y}{k} - \dfrac{y}{\omega} & \dfrac{ik}{\omega} - \dfrac{i\omega}{k} \\ y\left(\dfrac{ik}{\omega} - \dfrac{i\omega}{k}\right) - \partial_y\left(\dfrac{\partial_y}{k} - \dfrac{y}{\omega}\right) - i\delta^2\omega\left(\dfrac{ik}{\omega} - \dfrac{i\omega}{k}\right) & & 0 \\ i(k^2-\omega^2) & k\partial_y - \omega y & 0 \end{pmatrix}\begin{pmatrix} \hat{u} \\ \hat{v} \\ \hat{\eta} \end{pmatrix} = 0, \tag{7}$$

it follows from the third row that

$$i\left(k^2-\omega^2\right)\hat{u} = \left(\omega y - k\partial_y\right)\hat{v}. \tag{8}$$

Substitution of (8) into the second row of the matrix leads to:

$$y\left(\frac{y}{k} - \frac{d_y}{\omega}\right)\hat{v} - \left(\frac{d_{yy}}{k} - \frac{1}{\omega} - \frac{yd_y}{\omega} - k\delta^2 + \delta^2\frac{\omega^2}{k}\right)\hat{v} = 0. \tag{9}$$

Re-arranging (9) yields

$$\frac{d^2\hat{v}}{dy^2} + \left(\delta^2\omega^2 - \delta^2k^2 - \frac{k}{\omega} - y^2\right)\hat{v} = 0. \tag{10}$$

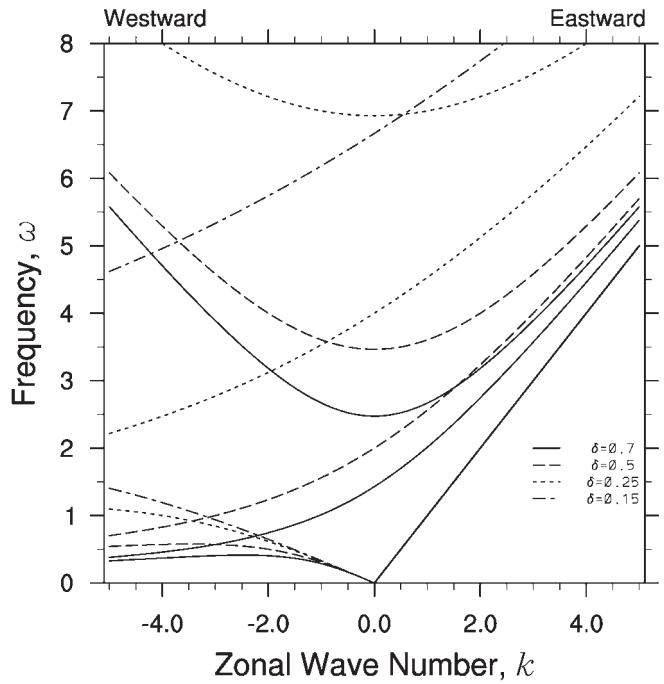

Figure 1. δ-modified equatorial waves, Rossby and inertio-gravity waves, for fixed $n=1$ (symmetric), Kelvin $n=-1$ and mixed Rossby $n=0$. All the waves are for $H=250$m, corresponding to the atmosphere first baroclinic mode. Frequencies and zonal wavenumbers are truncated in the display to 8 and 5 respectively.

Boundary conditions require vanishing solutions as $|y|\to\infty$. Thus, (10) results in the well known second order differential equation for decaying Hermite polynomials [see *Hochstrasser*, 1972]. Solutions of (10) are given by

$$\hat{v}_n(y) = \psi_n(y) = \frac{H_n(y)}{\left(2^n n!\pi^{1/2}\right)^{1/2}}e^{-y^2/2}, \tag{11}$$

with ψ_n being the Hermite functions and H_n the Hermite polynomials. The problem of finding the eigenfrequencies is reduced to the algebraic equation (12)

$$\delta^2\omega^2 - \delta^2k^2 - \frac{k}{\omega} = 2n+1, \tag{12}$$

with n a non-negative integer given by $n=\{0,1,2,\ldots\}$. There is a special case for the equatorial waves known as Kelvin wave. These modes are characterized by being meridionally geostrophic but zonally ageostrophic. Although this mode can not be obtained from the (7)–(10), it can be recovered by using $n=-1$ in the dispersion relation (12), as will be shown in subsequent sections.

Equation (12) gives up to three different solutions for ω for k,n, and δ specified. To obtain analytic expressions for these solutions, we shall use the limiting cases that are frequently found in the bibliography [*Matsuno*, 1966; *Wheeler*, 2002]. However, numerical solutions of the parametric dispersion relation (12) were also computed. The results are displayed in Figures 1 and 2. Although the

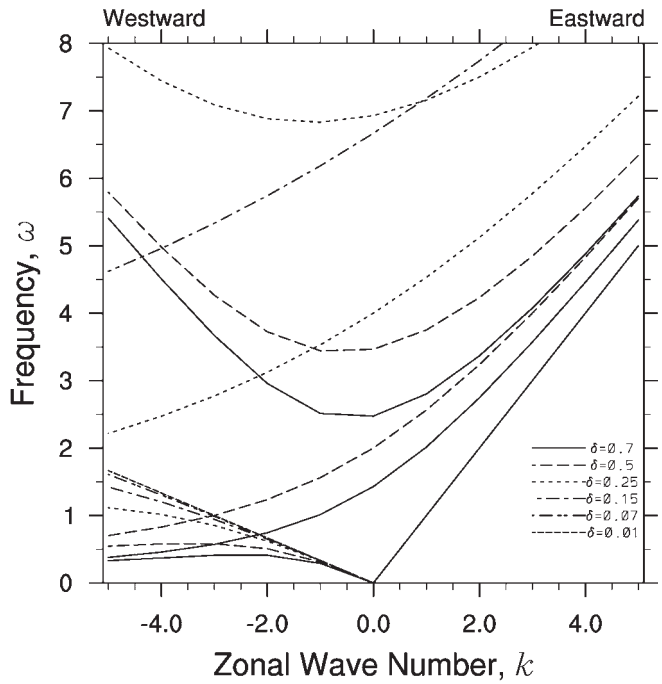

Figure 2. Numerically computed δ-modified equatorial waves, Rossby and inertio-gravity waves, for fixed $n=1$ (symmetric), Kelvin $n=-1$ and mixed Rossby $n=0$. All the waves are for $H=250$m, corresponding to the atmosphere first baroclinic mode. Frequencies and zonal wavenumbers are truncated in the display to 8 and 5 respectively.

eastward/westward asymmetry of the inertio-gravity waves are not captured in the limiting case, the dependency of the equatorial waves on the δ parameter seems to be well represented. Thus, we will use the analytic expressions for our subsequent analysis.

3.1. Slowness Space

Some other properties of the family of anisotropic equatorial waves can be readily seen if we use the slowness space [*Ripa*, 1982, 1983a, 1983b]. In the slowness space the square of the eigenfrequency (ω^2) is a simpler function of the slowness parameter $s=(k/\omega)$ than of the zonal wavenumber k. Furthermore, the equatorial wave types are more clearly distinguishable in slowness space, as can be seen in Figure 3. The dispersion relation in the slowness δ-space is given by

$$\omega^2=\frac{2n+1+s}{\delta^2(1-s^2)}. \tag{13}$$

When $\delta=1$, the slowness dispersion relation of *Ripa* [1982, 1983a, 1983b] is recovered. The equatorial waves in slowness space are displayed schematically in Figure 3, where the anisotropic (δ-dependent) equatorial wave types are displayed in terms of sC, with C, the first baroclinic wave speed and $s=\left(1/c_p^{(\delta)}\right)$ the reciprocal of the δ dependant phase speed $c_p^{(\delta)}$.

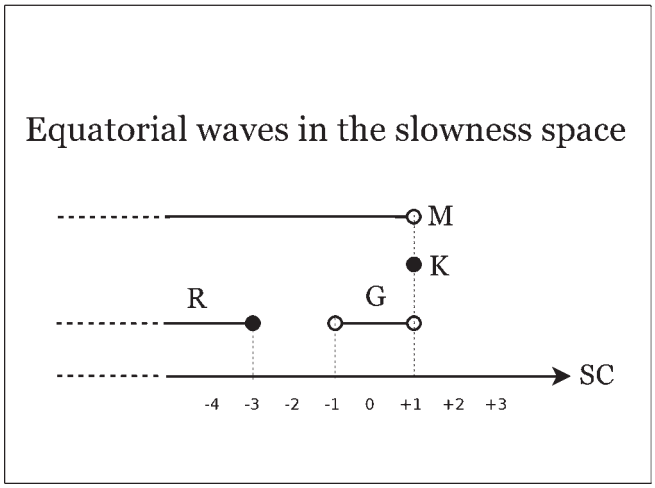

Figure 3. Schematic dispersion diagram for the β plane equatorial waves in the $\delta=1$ dimensional slowness space. The dispersion relation used is: $\omega^2=\beta c(2n+1+sC)/\left(1-(sC)^2\right)$ where c represents the velocity of the fastest allowed baroclinic mode for a given equivalent depth. The different equatorial waves are labeled by R Rossby, G inertio-gravity, K kelvin, M mixed Rossby-gravity wave. Open circle means asymptotic convergence. M and eastward G waves asymptotically converge towards the K wave speed (c). Westward G waves converge towards $-c$. The fastest R wave is three times slower than $-c$. M waves connects R and G modes.

3.2. The δ-Inertio-gravity Waves

For the high frequencies ($\frac{k}{\omega}\ll 1$), (12) reduces to

$$\omega^2\approx\frac{2n+1}{\delta^2}+k^2, \tag{14}$$

which is the dispersion relation for δ-modified inertio-gravity waves (or δ-modified Poincaré waves). Figure 4 displays the δ-inertio-gravity waves for $n=1$ and the equivalent depth of the first baroclinic mode. Note that as $\delta\to 0$, ω grows rapidly for any value of k. The larger the anisotropy (smaller δ), the larger the gravity wave frequency. It is also possible to note by comparing Figures 1, 4, and 5 that inertio-gravity dispersion curves become less convex as ω increases.

3.2.1. Spectral Occupation and Asymptotic Limits

The δ-inertio-gravity wave phase speed ($c_p^{(\delta)}$) is given by

$$c_p^{(\delta)}=\sqrt{\frac{2n+1}{\delta^2k^2}+1}. \tag{15}$$

Asymptotic limits for (15) as $k\to\infty$ are given by

$$\lim_{k\to\infty}c_p^{(\delta)}=\begin{cases}\infty & (\textit{for } \delta\to 0 \textit{ faster than } k\to\infty),\\ 1 & (\textit{for } k\to\infty \textit{ faster than } \delta\to 0).\end{cases} \tag{16}$$

Thus, for dominant values of anisotropy, the inertio-gravity phase speed becomes very large. The second case reveals asymptotic convergence towards the non-dimen-

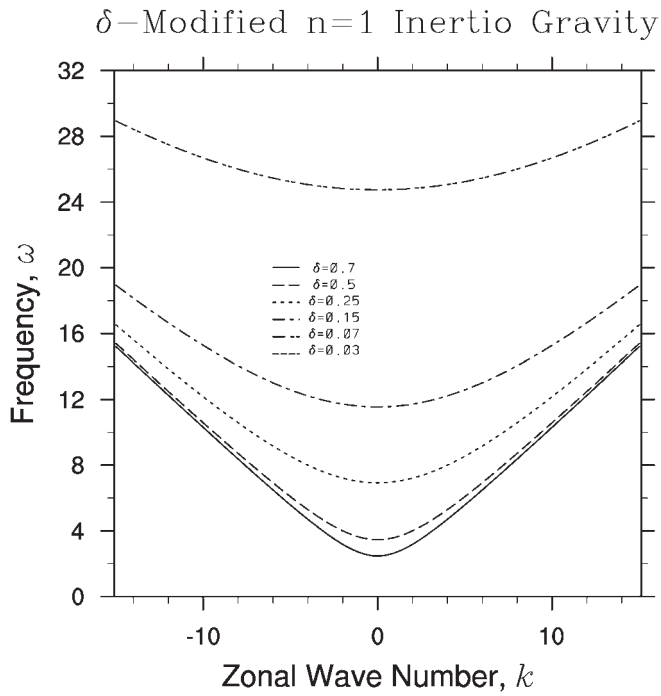

Figure 4. δ-modified equatorial inertio-gravity wave for fixed $n=1$, $H=250$m (first baroclinic mode).

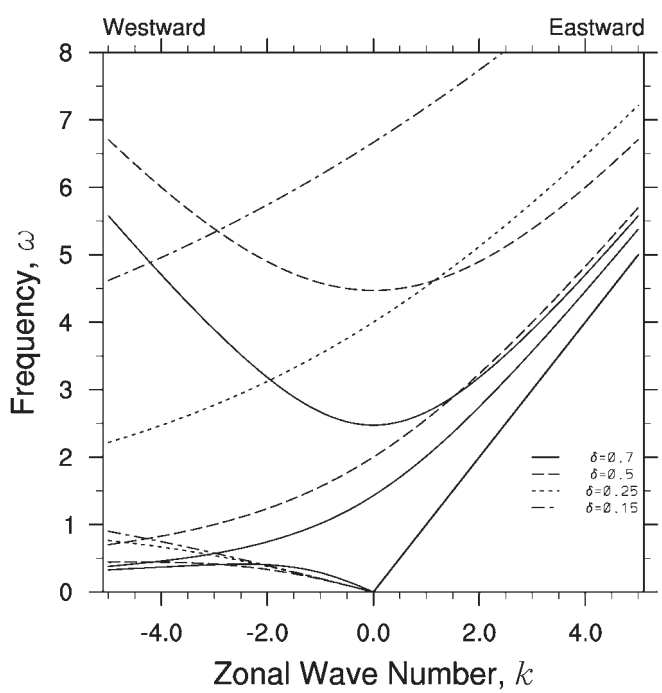

Figure 5. δ-modified equatorial waves, Rossby and inertio-gravity waves are for fixed $n=2$ (asymmetric), Kelvin $n=-1$ and mixed Rossby $n=0$. All the waves are for $H=250$m, corresponding to the atmosphere first baroclinic mode. Frequencies and zonal wavenumbers are truncated to 8 and 5 respectively.

sional fastest baroclinic mode phase speed. The eigenfrequency of the anisotropic Poincaré modes is given by

$$\omega^{(\delta)} = kc_p^{(\delta)} = \sqrt{\frac{2n+1}{\delta^2} + k^2}. \tag{17}$$

For $k=0$, the rate of growth due to the anisotropy is $1/\delta$. To estimate the value of $\omega^{(\delta)}$ for large values of k and small values of δ, it is possible to approximate $\omega^{(\delta)}$ by

$$\omega^{(\delta)} \approx (2n+1)^{1/4}\sqrt{\frac{2k}{\delta}}. \tag{18}$$

Thus, for $k \neq 0$, $\omega^{(\delta)}$ increases at a rate of $1/\sqrt{\delta}$. Since $1/\delta > 1/\sqrt{\delta}$, as was already noted, the eigenfrequency $\omega^{(\delta)}$ becomes less convex for smaller values of δ (Figure 4). Following (16), the slowness space parameter sC is also twofold as noted in

$$\lim_{k\to\infty} sC = \begin{cases} 0 & (\textit{for } \delta\to 0 \textit{ faster than } k\to\infty), \\ 1 & (\textit{for } k\to\infty \textit{ faster than } \delta\to 0). \end{cases} \tag{19}$$

In the first case, the δ inertio-gravity wave phase speed becomes very large for small values of δ, but is equal to the first baroclinic wave speed for large values of k. Further discussion about the slowness space parameter behavior in connection to the mixed Rossby-gravity waves is presented in the following sections.

3.3. The δ-Rossby Waves

Concerning the other limiting case of small frequencies ($\omega^2 \to 0$), (12) becomes

$$\omega \approx \frac{-k}{(2n+1)+\delta^2 k^2}, \tag{20}$$

which is the δ-modified equatorial Rossby wave dispersion relation. For small values of δ, the behavior of (20) is twofold. Thus, (20) converges to the non-dispersive Rossby wave frequency for small values of k, and tends to zero for large values of k. The precise inflection point of the dispersion curves of the Rossby waves is larger in absolute value as δ decreases. Precisely, when $\delta \to 0$ only a monotonic curve close to the non-dispersive Rossby wave is noted (see Figures 1, 6, and 7). This characteristic precludes the representation of short Rossby waves in the classical long wave approximation [*Ripa*, 1994; *Schubert et al.*, 2009].

3.3.1. Spectral Occupation and Asymptotic Limits

For Rossby waves $c_p^{(\delta)} = -1/\left(2n+1+\delta^2 k^2\right)$. Thus, taking $\delta=1$ the traditional phase speed is recovered ($c_p^{(\delta)} \equiv c_p$). For $k=0$, the $\delta=1$ phase speed $c_p = -1/(2n+1)$ and the $\max\left(c_p\right) = -1/3$ corresponds to $n=1$, which is the minimum meridional quantum number allowed. For any other n, $c_p \leq -1/3$. This upper limit is also valid for $c_p^{(\delta)} \leq -1/3$, implying that as $k \to 0$ the phase speed of the

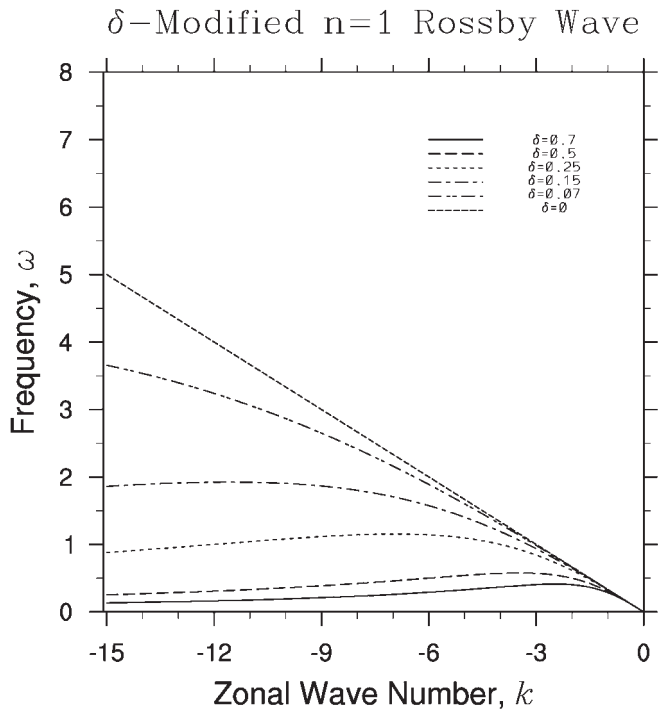

Figure 6. δ-modified equatorial Rossby wave for fixed $n=1$, $H=250$m (first baroclinic mode). The non-dispersive Rossby mode correspond to $\delta=0$.

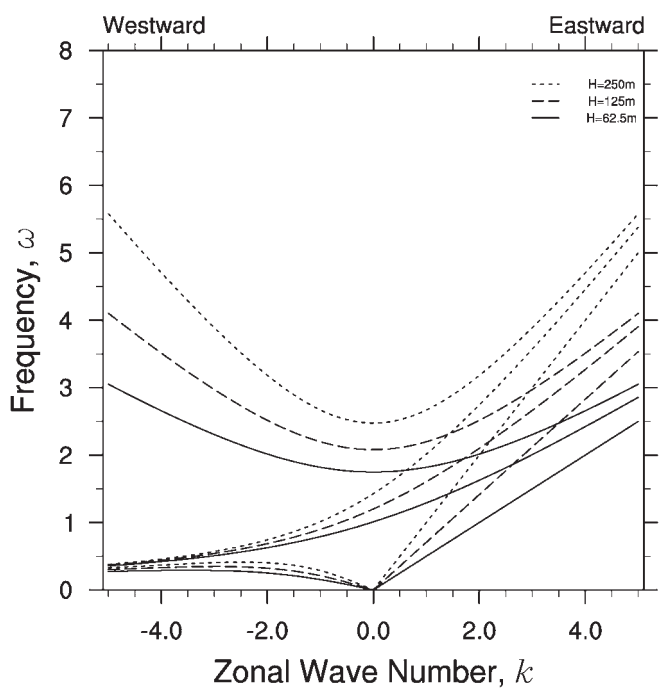

Figure 7. δ-modified Equatorial waves for varying $H=\{250,125,62.5\}$m; fixed $\delta=0.7$, and meridional quantum number $n=1$ for Rossby and inertio gravity waves, $n=0$ for mixed Rossby-gravity and $n=-1$ for Kelvin waves.

anisotropic Rossby waves is smaller than the phase speed of the nondispersive Rossby wave.

Conversely, for $k\to\infty$ we have:

$$\lim_{k\to\infty} c_p^{(\delta)} = \begin{cases} \dfrac{-1}{2n+1} & (\textit{for } \delta\to 0 \textit{ faster than } k\to\infty), \\ 0 & (\textit{for } k\to\infty \textit{ faster than } \delta\to 0). \end{cases} \tag{21}$$

For dominant values of δ, the nondispersive Rossby wave behavior of the phase speed is obtained. In contrast, for dominant values of k the phase speed tends to zero in agreement to what is obtained for traditional equatorial Rossby waves. Thus, the basic differences between the shallow water and the long wave approximation model in terms of Rossby waves are summarized in (21). The δ parameter dependency of the waves' phase speed makes somewhat elegant the passage from one limit to the other. In fact, it shows that it is possible to obtain convergence towards the phase speed of the ultra long Rossby waves even for increasingly large values of k depending on the δ that is at work (Figure 6). Similar results can be deduced using the dimensional slowness parameter (sC) defined by

$$sC = \begin{cases} -(2n+1) & (\textit{for } \delta\to 0 \textit{ faster than } k\to\infty) \\ -\infty & (\textit{for } k\to\infty \textit{ faster than } \delta\to 0). \end{cases} \tag{22}$$

3.4. The δ-Mixed Rossby Gravity (n = 0)

Using $n=0$ in the dispersion relation (12) and factoring $(\omega+k)$ yields

$$(\omega+k)\left(\omega^2-\omega k-\frac{1}{\delta^2}\right)=0. \tag{23}$$

The $\omega=-k$ solution does not satisfy the equatorial trapping boundary condition and, therefore, must be disregarded [*Matsuno*, 1966; *Moore et al.*, 1998; *Ripa*, 1994]. On the other hand, the quadratic polynomial factor in (23) determines two branches given by

$$\omega_\pm = \frac{1}{2}\left(k\pm\sqrt{k^2+\frac{4}{\delta^2}}\right). \tag{24}$$

These branches correspond to the dispersion relation of the $\delta-$mixed Rossby-gravity wave and its complex conjugate. Dispersion curves for the δ-modified equatorial waves can be found in Figures 1 and 5. The most outstanding effect of the anisotropy parameter δ is on the mixed Rossby-gravity waves, because it leads to the existence of a family of mixed Rossby-gravity waves. Thus, a family of connections of the slow and fast manifolds of the equatorial waves dynamics is introduced by the anisotropy.

3.4.1. Spectral Occupation and Asymptotic Limits

The mixed Rossby-gravity wave phase speed is given by $c_p^{(\delta)}=0.5\left(1+\sqrt{1+4/(\delta^2k^2)}\right)$. The asymptotic behavior of

$c_p^{(\delta)}$ is given by

$$\lim_{k\to\infty} c_p^{(\delta)} = \begin{cases} \infty & (\textit{for } \delta\to 0 \textit{ faster than } k\to\infty), \\ 1 & (\textit{for } k\to\infty \textit{ faster than } \delta\to 0). \end{cases} \tag{25}$$

Thus, sC also has a twofold limit that is exactly the same as in (19), i.e.,

$$\lim_{k\to\infty} sC = \begin{cases} 0 & (\textit{for } \delta\to 0 \textit{ faster than } k\to\infty), \\ 1 & (\textit{for } k\to\infty \textit{ faster than } \delta\to 0). \end{cases} \tag{26}$$

The eigenfrequency of the δ mixed Rossby-gravity wave-modes is given by $\omega = 0.5\left(k + \sqrt{k^2 + 4/\delta^2}\right)$. For $k\to 0$, the anisotropic eigen-frequency is proportional to $1/\delta$. The rate of increase is equal to that of the inertio-gravity waves. Further, comparing (25) and (26) with (16) and (19), one notes that the asymptotic behavior of mixed Rossby-gravity and inertio-gravity waves are also the same. Using the results displayed here together with the results of section 4.2, it is possible to conclude that the spectral space occupation, i.e., connection of 'slow' and 'fast' modes, is not lost with the anisotropy of the horizontal scales. The results presented here allow us to conclude that, even when equatorial waves of the shallow-water model are different from those of the long wave like approach, the differences can be properly parameterized using the anisotropy parameter δ. Thus, it is possible to infer the existence of an asymptotic completeness of the long wave model solutions.

3.5. The δ-Kelvin Wave

Another wave that is not formally obtained from equation (12), but can be recovered from it by choosing $n = -1$ is the Kelvin wave. Its dispersion relation is given by

$$\omega = k. \tag{27}$$

The meridional structure for Kelvin waves is given by $\hat{u}(y) = \hat{\eta}(y) = \hat{u}(0)e^{-y^2/2}$; $\hat{v}(y) = 0$. It is interesting to note that Kelvin waves are not modified by the anisotropy, because (27) is invariant under the transformation:

$$\delta\omega \to \omega, \tag{28a}$$

$$\delta k \to k. \tag{28b}$$

This invariance has implications for nonlinear interactions in the equatorial wave-guide, as will be pointed out below.

4. Family of Anisotropic Equatorial Shallow Water Waves

4.1. Analysis of the Spectrum

Figure 1 displays the family of equatorial waves that are obtained for some values of the anisotropy parameter δ. The selected values of the anisotropy parameter are representative of the ratio v/u in the tropical wave guide (e.g., $u = 20\text{m/s}, v = 5\text{m/s}$ (in the atmosphere) or $u = 1.0\text{m/s}$, $v = 0.25\text{m/s}$ (in the ocean) gives $\delta = 0.25$). Both δ-inertio-gravity and δ-Rossby waves resemble their shallow-water counterparts for some values of n (meridional quantum number), though differences are noticeable through careful inspection. Inertio-gravity waves become higher in frequency for increasing values of n. Conversely, δ-inertio-gravity waves are shifted to higher frequencies for decreasing values of δ. This can be more easily seen if one looks at the inflection point that divides eastward and westward inertio-gravity wave dispersion curves. For δ-Rossby waves, as δ increases (decreases) the modes tend to be more (less) restricted in the frequency domain. For δ-mixed Rossby-gravity waves it is possible to note that as δ diminishes, the mixed-Rossby waves are shifted to higher frequencies. This makes δ-mixed Rossby-gravity waves cross other waves' dispersion curves. Precisely, this behavior makes possible new connections of either: **a)** Rossby waves of different δ's, **b)** inertio-gravity waves of different δ's or **c)** both, Rossby and gravity waves of different δ's. The crossing points occur mainly to the left of the Kelvin wave dispersion curve. The Kelvin wave is a special case as it is invariant under the scaling (28). Thus, Kelvin waves of different δ's all coincide. The crossing curves are an indication that the anisotropic nonlinear equations (4) allow a broader spectrum of horizontal resonant wave interactions (nonlinear N-wave interactions, resonant interactions with harmonics, etc) than the nonlinear shallow-water equations studied by *Ripa* [1983a] and *Raupp and Silva Dias* [2006]. The many scales involved in the intersecting curves also suggest the possibility of the existence of shallow water turbulence in the domain of varying δ (chains of interacting waves/clusters of resonant wave triads). For the sake of illustration, in Figure 1 it can be noted for the window selected that the $\delta = 0.25$ mixed Rossby-gravity dispersion curve connects the $\delta = 0.7$ and 0.5 symmetric $n = 1$ westward inertio-gravity waves. Other possible interaction involves the $\delta = 0.5$ mixed Rossby-gravity, $\delta = 0.7$ eastward gravity and the $\delta = 0.15$ and 0.25 $n = 1$ Rossby waves. The impact of δ in nonlinear resonant three wave interactions of anisotropic equatorial waves was studied by *Ramírez Gutiérrez et al.* [2011].

4.2. Spectral Space Occupation

Recall that the equatorial β-plane is distinguished from the mid-latitude β-plane, because the frequency spectrum is fully occupied by the presence of the mixed Rossby-gravity waves. The mixed Rossby-gravity wave connects fast (inertio-gravity) and slow (Rossby) manifolds of the equatorial region. This is an aspect that is not observed in the mid-latitude β-plane, as was pointed out by *Matsuno* [1966]. The connection between slow and fast manifolds is possible because there exists a critical wavenumber $k = k_{Cr}$ such that for $k < k_{Cr}$ ($k > k_{Cr}$) the mixed Rossby-gravity wave behaves

as a Rossby (inertio-gravity) wave. Moreover, this critical k_{Cr} is connected with $\partial\omega/\partial k=0$ for both Rossby and inertio-gravity waves [*Pedlosky*, 1987; *Cane and Sarachik*, 1976]. Thus, if we compute the modification of the inflection point for the Rossby waves by the δ-parameter, and if it is at the same rate that the modification of the mixed Rossby-gravity waves, the distinguishing feature of the equatorial β-plane related to the connection between the fast and slow manifolds is not lost with the inclusion of the anisotropy between zonal and meridional scales. To demonstrate this, let us compute the inflection point for the Rossby wave via

$$\frac{\partial\omega}{\partial k}=\frac{k^2\delta^2-(2n+1)}{\left((2n+1)+\delta^2k^2\right)^2}=0, \tag{29}$$

so that

$$k_{Cr}=-\frac{(2n+1)^{1/2}}{\delta} \tag{30}$$

and

$$\omega_{max}(k)\equiv\omega(k_{Cr})=\frac{1}{2\delta(2n+1)^{1/2}}. \tag{31}$$

For fixed n, as δ decreases, k_{Cr} decreases (larger in absolute values), whereas $\omega(k_{Cr})$ increases. The growth rate of $\omega(k_{Cr})$ is similar to the growth rate of the mixed Rossby-gravity wave ($\sim 1/(2\delta)$). Thus, the connection between the slow and fast modes is preserved by the effect of the anisotropy of the scalings. Furthermore the ratio $\omega_{\text{mixed}}/\omega_{\text{Rossby}}$ is given by

$$\left(\frac{\omega_{\text{mixed}}}{\omega_{\text{Rossby}}}\right)_{|k=k_{Cr}}=\left[-(2n+1)^{1/2}\pm(2n+1+4)^{1/2}\right](2n+1)^{1/2}, \tag{32}$$

and is independent of δ, which means that their growth rates are always proportional to each other. On the other hand, for Rossby waves at fixed values δ, the well known behavior of the dispersion curves is recovered. For instance, as n increases k_{Cr} decreases and $\omega_{max}(k)\equiv\omega(k_{Cr})$ decreases.

The results presented here suggest that the full frequency occupation in wavenumber continues to be valid in the equatorial β-plane region for values of δ smaller than one (anisotropic scalings). Furthermore, small values of δ are physically more reasonable than $\delta=0$, as is typically used in the long wave approximation. This feature suggests that completeness in the long wave approximation can only be attained if we re-include the inertio-gravity and mixed Rossby-gravity waves. Implications for the nonlinear wave-wave interactions are analyzed in the next section.

5. Resonant Triads in the Anisotropic Shallow Water Model

To determine the number of nonlinearly interacting resonant triads allowed by (4), it is necessary to use the resonance conditions in the dispersion relation of one of the triad members. This leads to a family of polynomials labeled by δ. The procedure is explained as follows. First of all we define the variables $N_a=2\eta_a+1+s_a$ and $D_a=1-s_a^2$. The dimensionless dispersion relation can be re-written as

$$\omega_a^2=\frac{N_a}{\delta_a^2D_a}. \tag{33}$$

The subscript (a) labels any of the triad members. The other two members are labeled by (c) and (b). The conditions for resonance are $\omega_c=\omega_a+\omega_b$ and $\omega_c s_c=\omega_a s_a+\omega_b s_b$, respectively. The second condition is the slowness space representation of $k_c=k_a+k_b$. Introducing resonance conditions into (33) we obtain

$$\delta_c^2(\omega_a+\omega_b)^2-\delta_c^2(\omega_a s_a+\omega_b s_b)^2=N_c. \tag{34}$$

Performing binomial expansions and using (33) for waves a and b; and then re-arranging equation (34) we obtain

$$2\delta_c^2\omega_a\omega_b(1-s_as_b)=\left(N_c-\delta_c^2N_a/\delta_a^2-\delta_c^2N_b/\delta_b^2\right). \tag{35}$$

Let (c) be the member with the intermediate slowness of the triad. Thus, this is the wave that gives/receives energy to/from the other two components. In such a case its slowness is given by

$$s_c=\frac{s_a\omega_a+s_b\omega_b}{\omega_a+\omega_b}. \tag{36}$$

Using equation (36) together with the definition of N_c in equation (35) and then factoring ω_a and ω_b, we obtain

$$\left[\delta_c^2\{2\omega_a\omega_b(1-s_as_b)\}-2\left(n_c-\frac{\delta_c^2n_a}{\delta_a^2}-\frac{\delta_c^2n_b}{\delta_b^2}\right)-\left(1-\frac{\delta_c^2}{\delta_a^2}-\frac{\delta_c^2}{\delta_b^2}\right)-s_a+\delta_c^2\left(\frac{s_a}{\delta_a^2}+\frac{s_b}{\delta_b^2}\right)\right]\omega_a=$$
$$-\left[\delta_c^2\{2\omega_a\omega_b(1-s_as_b)\}-2\left(n_c-\frac{\delta_c^2n_a}{\delta_a^2}-\frac{\delta_c^2n_b}{\delta_b^2}\right)-\left(1-\frac{\delta_c^2}{\delta_a^2}-\frac{\delta_c^2}{\delta_b^2}\right)-s_b+\delta_c^2\left(\frac{s_a}{\delta_a^2}+\frac{s_b}{\delta_b^2}\right)\right]\omega_b.$$

Multiplying all the terms in (37) by D_aD_b, re-arranging the first term of each side of the equality sign, then squaring both sides and using (33) for the labels a and b to eliminate the ω dependency, we get

$$\left[\delta_c^2\left[\frac{2N_b}{\delta_b^2}(1-s_as_b)\right]-D_bB_{ba}\right]^2\frac{N_aD_a}{\delta_a^2}=$$
$$\left[\delta_c^2\left[\frac{2N_a}{\delta_a^2}(1-s_as_b)\right]-D_aB_{ab}\right]^2\frac{N_bD_b}{\delta_b^2}, \tag{37}$$

where,

$$B_{ab}=2\left[n_c-\frac{\delta_c^2n_a}{\delta_a^2}-\frac{\delta_c^2n_b}{\delta_b}\right]+\left[1-\frac{\delta_c^2}{\delta_a^2}-\frac{\delta_c^2}{\delta_b^2}\right]+$$
$$s_a-\delta_c^2\left(\frac{s_a}{\delta_a^2}+\frac{s_b}{\delta_b^2}\right), \tag{38}$$

and B_{ba} is obtained by exchanging $a\leftrightarrow b$. Thus,

$$F(s_a,s_b;\delta_a;\delta_b;\delta_c)=\left[\delta_c^2\left[\frac{2N_b}{\delta_b^2}(1-s_as_b)\right]-D_bB_{ba}\right]^2\frac{N_aD_a}{\delta_a^2}-$$
$$\left[\delta_c^2\left[\frac{2N_a}{\delta_a^2}(1-s_as_b)\right]-D_aB_{ab}\right]^2\frac{N_bD_b}{\delta_b^2}=0. \tag{39}$$

To solve (39) it is necessary to fix the three δ parameters and one of the slowness parameters. Even so, the resulting polynomial is of the 9th degree in s. This gives us an idea of the complexity of the problem of finding resonant triads.

For the case of $\delta=\delta_a=\delta_b=\delta_c$; B_{ab} is independent of δ and $F(s_a,s_b;\delta_a;\delta_b;\delta_c)$ becomes

$$F(s_a,s_b;\delta)=\frac{F(s_a,s_b)}{\delta^2}=\left[[2N_b(1-s_as_b)]-D_bB_{ba}\right]^2\frac{N_aD_a}{\delta^2}-$$
$$\left[[2N_a(1-s_as_b)]-D_aB_{ab}\right]^2\frac{N_bD_b}{\delta^2}=0. \tag{40}$$

Thus, for interacting waves within the same anisotropic family, the number of different possible interactions is independent of δ. However, for interacting waves of different families, the anisotropy must be considered. The polynomial $F(s_a,s_b)$ was studied by *Ripa* [1983a], who found nineteen different types of triad interactions. The results of *Ripa* [1983a] are equivalent to solving (39) for a fixed δ.

6. Family of Waves for Varying Vertical Structures and Anisotropy

Finally, in this section we extend the anisotropic shallow water waves to the equatorial primitive equations with discrete vertical structures. The dispersion relation used to plot Figure 7 was computed following the methodology described in the previous sections, but starting from the equatorial primitive equations subjected to rigid vertical boundary conditions. The specific expression is written in (41), where m^2 is the separation constant of the vertical and horizontal structures. A derivation of this expression depending on m, but not on δ, is given by *Pedlosky* [1987] (Chapter 8). Here the same equation, but with the explicit dependency on δ, is given by

$$\delta^2\omega^2m-\frac{\delta^2k^2}{m}-\frac{k}{m\omega}=2n+1. \tag{41}$$

It is worth mentioning that under the transformation $(\delta\omega m^{1/2}\rightarrow\omega)$; $(\delta k/m^{1/2}\rightarrow k)$ the traditional dispersion relation is recovered, that is, $\omega^2-k^2-k/\omega=2n+1$. This point is associated with the fact that the shallow water model is valid for the different baroclinic structures with the proper equivalent depth.

Figure 7 displays part of the wave families obtained by varying the equivalent depth ($\bar{H}$), while keeping $\delta=0.7$ fixed. In contrast to previous sections, a modification of the Kelvin wave is noted; this is due to its dimensional dispersion relation $\omega=\sqrt{g\bar{H}}k$. Crossing curves occur near the Kelvin wave and the involved modes are the mixed Rossby-gravity, Kelvin and Eastward inertio-gravity waves. The overlapping of the curves is indicative of the existence of resonant wave interactions of the scattering type involving equatorial waves associated with different vertical structures, since each intersection establishes a resonant triad composed of a zonally symmetric geostrophic mode and the modes associated with the intercepting dispersion curves. In this type of interaction, the zero-frequency mode allows the two propagating waves to exchange energy but is unaffected by the interacting modes [*Raupp and Silva Dias*, 2006]. It is noticeable that by varying $\bar{H}$, inertio-gravity waves are modified in such a way that they tend to diverge from each other at larger k's, in contrast to what is obtained by varying δ, where inertio-gravity waves tend to converge (compare with Figure 1). Although not shown, it can also be noted that there is an overlapping of both families: the vertically varying and the anisotropic equatorial waves for several wavenumbers and frequencies. Due to the association of these intersections with scattering resonant triad interactions, the overlapping of both families suggests the possibility of the existence of a large number of triads in the anisotropically scaled equatorial primitive equations. Also, the intersections might suggest a possible tendency for a more symmetric wave turbulence spectrum, since the elastic scattering interactions act in general to symmetrize the spectrum of weakly interacting waves [*McComas and Bretherton*, 1977]. Nonetheless, due to the high number of degrees of freedom associated with the interaction spectrum, it is not trivial to predict the statistical equilibrium state of the interacting modes to the full extent of all the interactions, except probably by means of numerical computations. However, some recent works suggest that key features of phenomena like the MJO, El Niño, and the PDO can be explained as the result of a restricted set of horizontal and vertical interacting modes [*Raupp and Silva Dias*, 2006, 2009; *Ramírez Gutiérrez and Silva Dias*, 2009; *Kartashova and L'vov*, 2007]. In addition, the long wave model has been

used in theoretical multi-scale models of the MJO and convectively coupled equatorial waves [*Biello and Majda*, 2005; *Majda and Stechmann*, 2009; *Klein and Majda*, 2006], and references therein. Thus, the results presented here can contribute to better understanding of the nonlinear interactions in a context more related to the tropical region, where anisotropy is predominant.

7. Concluding Remarks

The anisotropic shallow water model (4) represents an intermediate regime between the shallow water and the long wave equation models. The asymptotic limits of the anisotropic shallow water model are the shallow water equations for $\delta = 1$ and the long wave equations for $\delta = 0$. It was shown in the present work that the transition from one regime to the other can also be verified in the dispersion relation of the δ-modified equatorial Rossby wave. For moderate to large values of δ, the anisotropic Rossby wave dispersion relation tends to the non-dispersive Rossby wave (westward propagating) dispersion curve for small values of the zonal wave number k, and tends to the dispersive Rossby wave (eastward propagating) for large values of the zonal wavenumber. However, for small values of δ (close to zero), the Rossby wave only tends to the non-dispersive Rossby wave regime, irrespective of the value of the zonal wave number (k). In fact, Rossby waves for small values of δ are bending towards their asymptotic limit at a rate of $1/2\delta$ (computed at the critical wavenumber k_{C_r}). The critical wavenumber represents the inflection point that divides eastward (dispersive Rossby) and westward (non-dispersive) Rossby waves. The critical wavenumber was computed for the anisotropic shallow water model and it was found that k_{C_r} is also a function of $1/\delta$. Thus, as δ decreases, the k_{C_r} becomes large in absolute value, yielding the enlargement of the frequency spectrum of the non-dispersive Rossby waves. As a consequence, in the limiting case $\delta = 0$, only non-dispersive Rossby waves are allowed.

Notwithstanding, for values of δ computed for typical values of the scales found in the tropical region, both mixed Rossby-gravity and inertio-gravity waves must be re-included to complete the set of orthonormal basis functions. The completeness allows exact representation of any state of the model, which constitutes a required property for nonlinear interaction studies. The computation of the dispersion relation for all the waves reveals that, with the exception of the Kelvin wave, all the modes are modified by the δ parameter. As discussed in this paper, the predominant characteristic is that the mixed Rossby-gravity and the inertio-gravity modes are shifted to higher frequencies as δ decreases. It was found that even when the δ mixed Rossby-gravity wave is shifted to higher frequencies, it continues to connect slow and fast manifolds. The ratio between the δ-Rossby and δ-mixed Rossby-gravity wave frequencies computed at k_{C_r} is independent of δ. An important point of our analysis that has not been previously found is that the anisotropy of the zonal and meridional spatial scales produces a family of mixed Rossby-gravity waves that enables new possible connections between slow and fast manifolds. The connections are represented by intersections of the dispersion curves. Thus, all the new dispersion curve intersections are indicative of the possibility of new non-linear wave-wave interactions. To verify the implications of the anisotropic scalings for non-linear wave-wave interactions, we have computed the nonlinear resonant triad interaction condition for the δ-modified equatorial wave modes. Following the approach of *Ripa* [1983a] for the isotropic shallow-water equatorial waves, we have used the dispersion relation to express the resonance condition in terms of a polynomial that determines the number of resonant triads. The polynomial determines the possible resonant triads for the general case of interacting families (different δ's) of equatorial waves if the three δ parameters and one of the interacting modes are fixed. The resulting polynomial is of nine degree in the slowness space parameter. This approach gives an idea of the complexity and diversity of possible new resonant triad interactions. For the special case of interacting modes of the same anisotropic family, the polynomial reduces to the same polynomial found by *Ripa* [1983a], which has nineteen different types/combinations of triads. Due to the fact that the δ parameter represents different space and time scales, the results obtained here have a potential application for multi-scale nonlinear interactions. The asymptotic nature of the long-wave model solutions obtained from the complete shallow water model solutions guarantee the exact representation of any state. *Ramírez Gutiérrez et al.* [2011] studied the nonlinear interactions for realistic though conservative estimates of δ. In their approach, the dispersion properties, as well as the spatial structure of the equatorial wave modes, were assumed to be unaffected by the anisotropy parameter, with the anisotropy modifying only the nonlinear interactions among the isotropic eigenmodes. They found that there is an effective modification of both the nonlinear slow energy and amplitude modulations in the anisotropic resonant triad interactions.

In some earlier studies on equatorial wave response to prescribed forcings, there were indications of the existence of the family of anisotropic equatorial waves [e.g., *Gill*, 1980; *Zebiak*, 1982; *Webster*, 1972; *Silva Dias et al.*, 1988]. However, in those studies the results were linked to the response to a prescribed forcing. Here, an unforced model was used and the results reveal that the anisotropy introduces modifications in both the dispersive properties of the waves and their nonlinear wave-wave interactions. The asymptotic method adopted here also avoids the introduction of an approximation to the local time derivative of the meridional momentum equation used by *Schubert et al.* [2009] to break the strictly meridional geostrophic balance implied in the long wave approximation.

The anisotropy was also considered for the case of the dispersion relation of the stratified primitive equation

model. In this case, crossing curves occur near the Kelvin wave and the involved modes are the mixed Rossby-gravity, Eastward inertio-gravity and the Kelvin waves. Once again, the overlapping of the curves is indicative of at least the existence of resonant wave interactions of the scattering type (zonally symmetric geostrophic mode and the dispersive modes associated with the intercepting curves). There was found an overlapping of both families, the vertically varying and the anisotropically scaled shallow water wave modes, suggesting the existence of a larger number of triads and probably a more symmetric wave turbulence spectrum in the anisotropic equatorial wave dynamics. Although it is not trivial to predict the statistical equilibrium state produced by all the possible non-linear interactions, it is argued that this state might be close to the dominant modes of the tropical variability associated with the MJO, El Niño, and the PDO.

Acknowledgments. We would like to thank to the Fundação de Amparo à Pesquisa do Estado de São Paulo (FAPESP) for financial support. This work is contribution to the INCT for Climate Change and to the REDECLIMA project. We thank the reviewers and Wayne Schubert for the suggestions that greatly improved this paper. The first author is grateful to Rosio Camayo for her help and comments.

References

Biello, J. A., and A. J. Majda (2005), A new multiscale model for the Madden-Julian Oscillation, *J. Atmos. Sci.*, *62*, 1694–1721, doi:10.1175/JAS3455.1.

Cane, M., and E. Sarachik (1976), Forced baroclinic ocean motions I: The linear equatorial unbounded case, *J. Mar. Res.*, *34*, 629–665.

Dijkstra, H. (2000), Nonlinear Physical Oceanography: A Dynamical Systems Approach to the Large Scale Ocean Circulation and El Niño, Atmos. *Oceangr. Sci. Libr.*, vol. *22*, Kluwer Acad., Boston, Mass.

Gill, A. (1980), Some simple solutions for heat-induced tropical circulation, *Q. J. R. Meteorol. Soc.*, *106*, 447–462, doi:10.1002/qj.49710644905.

Gill, A., and P. Phlips (1986), Nonlinear effects on heat-induced circulation of the tropical atmosphere, *Q. J. R. Meteorol. Soc.*, *112*, 69–91, doi:10.1002/qj.49711247105.

Hochstrasser, W. (1972), Orthogonal polynomials, in Handbook of Math Functions With Formulas, Graphs, and Mathematical Tables, *Appl. Math. Ser.*, vol. *55*, pp. 771–802, U.S. Dep. of Commer., Natl. Bur. of Stand., Washington, D. C.

Kartashova, E., and V. L'vov (2007), Model of intraseasonal oscillations in Earth's atmosphere, *Phys. Rev. Lett.*, *98*, 198501, doi:10.1103/PhysRevLett.98.198501.

Khouider, B., and A. Majda (2006), A Simple multicloud parameterization for convectively coupled tropical waves. Part I: Linear analysis, *J. Atmos. Sci.*, *63*, 1308–1323, doi:10.1175/JAS3677.1.

Khouider, B., and A. Majda (2007), A Simple multicloud parameterization for convectively coupled tropical waves. Part II: Nonlinear simulations, *J. Atmos. Sci.*, *64*, 381–400, doi:10.1175/JAS3833.1.

Klein, R., and A. Majda (2006), Systematic multiscale models for deep convection on mesoscales, *Theor. Comput. Fluid Dyn.*, *20*, 525–551, doi:10.1007/s00162-006-0027-9.

Majda, A. (2002), *Introduction to PDE's and Waves for the Atmosphere and Ocean, Courant Lect. Notes Math.*, vol. *9*, Courant Inst. of Math. Sci., New York.

Majda, A. J. (2007), New multiscale models and self-similarity in tropical convection, *J. Atmos. Sci.*, *64*, 1393–1404, doi:10.1175/JAS3880.1.

Majda, A. J., and R. Klein (2003), Systematic multiscale models for the Tropics, *J. Atmos. Sci.*, *60*, 393–408, doi:10.1175/1520-0469(2003)060<0393:SMMFTT>2.0.CO;2.

Majda, A. J., and S. Stechmann (2009), The skeleton of tropical intraseasonal oscillations, *Proc. Natl. Acad. Sci. U. S. A.*, *106*, 8417–8422, doi:10.1073/pnas.0903367106.

Matsuno, T. (1966), Quasi-geostrophic motions in the equatorial area, *J. Meteorol. Soc. Jpn.*, *44*, 25–42.

McComas, C., and F. Bretherton (1977), Resonant interaction of oceanic internal waves, *J. Geophys. Res.*, *82*, 1397–1412, doi:10.1029/JC082i009p01397.

McWilliams, J., and P. Gent (1978), A coupled air and sea model for the tropical Pacific, *J. Atmos. Sci.*, *35*, 962–989, doi:10.1175/1520-0469(1978)035<0962:ACAASM>2.0.CO;2.

McWilliams, J., and P. Gent (1980), Intermediate models of planetary circulations in the atmosphere and ocean, *J. Atmos. Sci.*, *37*, 1657–1678, doi:10.1175/1520-0469(1980)037<1657:IMOPCI>2.0.CO;2.

Moore, D. W., R. C. Kloosterziel, and W. S. Kessler (1998), Evolution of mixed Rossby gravity waves, *J. Geophys. Res.*, *103*, 5331–5346, doi:10.1029/97JC02419.

Pedlosky, J. (1987), *Geophysical Fluid Dynamics,* Springer, New York, doi:10.1007/978-1-4612-4650-3.

Ramírez Gutiérrez, E., and P. L. Silva Dias (2009), Núcleo dinâmico de modelos balanceados da interação entre oceano e atmosfera, *An. CNMAC*, *2*, 479–480.

Ramírez Gutiérrez, E., P. L. Silva Dias, and C. Raupp (2011), Asymptotic approach for the nonlinear equatorial long wave interactions, *J. Phys. Conf. Ser.*, *285*(1), 012020, doi:10.1088/1742-6596/285/1/012020.

Raupp, C. F. M., and P. L. Silva Dias (2006), Dynamics of resonantly interacting equatorial waves, *Tellus, Ser. A*, *58*, 263–279, doi:10.1111/j.1600-0870.2006.00151.x.

Raupp, C. F. M., and P. L. Silva Dias (2009), Resonant wave interactions in the presence of a diurnally varying heat source, *J. Atmos. Sci.*, *66*, 3165–3183, doi:10.1175/2009JAS2899.1.

Ripa, P. (1982), Nonlinear wave-wave interactions in a one-layer reduced-gravity model on the equatorial β plane, *J. Phys. Oceanogr.*, *12*, 97–111, doi:10.1175/1520-0485(1982)012<0097:NWIIAO>2.0.CO;2.

Ripa, P. (1983a), Weak interactions of equatorial waves in a one-layer model. Part I: General properties, *J. Phys. Oceanogr.*, *13*, 1208–1226, doi:10.1175/1520-0485(1983)013<1208:WIOEWI>2.0.CO;2.

Ripa, P. (1983b), Weak interactions of equatorial waves in a one-layer model. Part II: Applications, *J. Phys. Oceanogr.*, *13*, 1227–1240, doi:10.1175/1520-0485(1983)013<1227:WIOEWI>2.0.CO;2.

Ripa, P. (1994), Horizontal wave propagation in the equatorial waveguide, *J. Fluid Mech.*, *271*, 267–284, doi:10.1017/S002211209400176X.

Schopf, P., and M. Suarez (1990), Ocean wave dynamics and the time scale of ENSO, *J. Phys. Oceanogr.*, *20*, 629–645, doi:10.1175/1520-0485(1990)020<0629:OWDATT>2.0.CO;2.

Schubert, W., L. Silvers, M. Masarik, and A. Gonzalez (2009), A filtered model of tropical wave motions, *J. Adv. Model. Earth Syst.*, *1*, 3., doi:10.3894/JAMES.2009.1.3

Silva Dias, P. L., W. H. Schubert, and MDeMaria (1988), Large scale response of the tropical atmosphere to transient convection, *J. Atmos. Sci.*, *45*, 549–566, doi:10.1175/1520-0469(1988)045<0549:VIACOM>2.0.CO;2.

Webster, P. (1972), Response of the tropical atmosphere to local steady forcing, *Mon. Weather Rev.*, *100*, 518–541, doi:10.1175/1520-0493(1972)100<0518:ROTTAT>2.3.CO;2.

Wheeler, M. (2002), Tropical meteorology: Equatorial waves, in *Encyclopedia of Atmospheric Sciences*, pp. 2313–2325, Academic, Amsterdam.

Zebiak, S. (1982), A simple atmospheric model of relevance to El Niño, *J. Atmos. Sci.*, *39*, 2017–2027, doi:10.1175/1520-0469(1982)039<2017:ASAMOR>2.0.CO;2.